mRNA Degradation Rates Are Coupled to Metabolic Status in *Mycobacterium smegmatis*

Diego A. Vargas-Blanco,[a] Ying Zhou,[a] L. Gregory Zamalloa,[a] Tim Antonelli,[b] Scarlet S. Shell[a,c]

[a]Department of Biology and Biotechnology, Worcester Polytechnic Institute, Worcester, Massachusetts, USA
[b]Department of Mathematics, Worcester State University, Worcester, Massachusetts, USA
[c]Program in Bioinformatics and Computational Biology, Worcester Polytechnic Institute, Worcester, Massachusetts, USA

ABSTRACT The success of *Mycobacterium tuberculosis* as a human pathogen is due in part to its ability to survive stress conditions, such as hypoxia or nutrient deprivation, by entering nongrowing states. In these low-metabolism states, *M. tuberculosis* can tolerate antibiotics and develop genetically encoded antibiotic resistance, making its metabolic adaptation to stress crucial for survival. Numerous bacteria, including *M. tuberculosis*, have been shown to reduce their rates of mRNA degradation under growth limitation and stress. While the existence of this response appears to be conserved across species, the underlying bacterial mRNA stabilization mechanisms remain unknown. To better understand the biology of nongrowing mycobacteria, we sought to identify the mechanistic basis of mRNA stabilization in the nonpathogenic model *Mycobacterium smegmatis*. We found that mRNA half-life was responsive to energy stress, with carbon starvation and hypoxia causing global mRNA stabilization. This global stabilization was rapidly reversed when hypoxia-adapted cultures were reexposed to oxygen, even in the absence of new transcription. The stringent response and RNase levels did not explain mRNA stabilization, nor did transcript abundance. This led us to hypothesize that metabolic changes during growth cessation impact the activities of degradation proteins, increasing mRNA stability. Indeed, bedaquiline and isoniazid, two drugs with opposing effects on cellular energy status, had opposite effects on mRNA half-lives in growth-arrested cells. Taken together, our results indicate that mRNA stability in mycobacteria is not directly regulated by growth status but rather is dependent on the status of energy metabolism.

IMPORTANCE The logistics of tuberculosis therapy are difficult, requiring multiple drugs for many months. *Mycobacterium tuberculosis* survives in part by entering nongrowing states in which it is metabolically less active and thus less susceptible to antibiotics. Basic knowledge on how *M. tuberculosis* survives during these low-metabolism states is incomplete, and we hypothesize that optimized energy resource management is important. Here, we report that slowed mRNA turnover is a common feature of mycobacteria under energy stress but is not dependent on the mechanisms that have generally been postulated in the literature. Finally, we found that mRNA stability and growth status can be decoupled by a drug that causes growth arrest but increases metabolic activity, indicating that mRNA stability responds to metabolic status rather than to growth rate *per se*. Our findings suggest a need to reorient studies of global mRNA stabilization to identify novel mechanisms that are presumably responsible.

KEYWORDS ATP, *Mycobacterium smegmatis*, carbon starvation, hypoxia, mRNA degradation, mRNA stability, stress response, tuberculosis, *Mycobacterium tuberculosis*

Most bacteria periodically face environments that are unfavorable for growth. To overcome such challenges, bacteria must tune their gene expression and energy usage. Regulation of mRNA turnover can contribute to both of these. However, the mechanisms by which mRNA turnover is carried out and regulated remain poorly understood, particularly in mycobacteria.

During infection, the human pathogen *Mycobacterium tuberculosis* faces not only the immune response and antibiotics but also nonoptimal microenvironments, such as hypoxia and starvation (1, 2). Regulation of mRNA turnover appears to contribute to adaptation to such conditions. A global study of mRNA decay in *M. tuberculosis* showed a dramatic increase in transcriptome stability (increased mRNA half-lives) in response to hypoxia, compared to that with aerobic growth (3). This suggests that mRNA stabilization contributes to energy conservation in the energy-limited environments that *M. tuberculosis* encounters during infection. Similar responses have been shown for other bacteria under conditions that slow or halt growth, including carbon deprivation, stationary phase, and temperature shock (4–13). However, the mechanisms responsible for global regulation of mRNA stability in prokaryotes remain unknown.

A conventional model for RNA decay in *Escherichia coli* starts with endonucleolytic cleavage by RNase E, particularly in 5'-end-monophosphorylated mRNAs (14–16). The resulting fragments are further cleaved by RNase E, producing fragments that are fully degraded by exonucleases, such as polynucleotide phosphorylase (PNPase), RNase II, and RNase R (17, 18). mRNA degradation is coordinated by the formation of a complex known as the degradosome. In *E. coli*, RNase E serves as the scaffold for degradosomes containing RNA helicases, the glycolytic enzyme enolase, and PNPase (19–23). Other organisms that encode RNase E form similar degradosomes (24, 25). In bacteria lacking RNase E, other endonucleases assume the scaffold function (26–28). Mycobacteria encode RNase E, but efforts to define the mycobacterial degradosome have produced inconsistent results (29, 30). It is unclear if degradosome reorganization or dissolution contribute to the global regulation of mRNA degradation in any bacteria. Interestingly, the importance of degradosome formation in *E. coli* varies depending on the carbon sources provided, suggesting links between RNA degradation and metabolic capabilities (31). Furthermore, the chaperones DnaK and CsdA associate with degradosomes in *E. coli* under certain stresses (20, 32, 33).

Global transcript stabilization in stressed bacteria may plausibly result from reduced RNase abundance, reduced RNase activity, and/or reduced accessibility of transcripts to degradation proteins. In *E. coli*, multiple stressors upregulate RNase R, possibly to mitigate ribosome misassembly (34, 35), and RNase III levels decrease under cold shock and stationary phase (36). Surprisingly, protein levels for most putative RNA degradation proteins in *M. tuberculosis* remain unaltered under hypoxic conditions (37), suggesting that mRNA degradation is not necessarily regulated at the level of RNase abundance in mycobacteria. However, there is evidence that RNase activity may be regulated. For example, proteins such as RraA and RraB can alter the function of the RNase E-based degradosome in *E. coli* (38). Translating ribosomes can mask mRNA cleavage sites and stabilize mRNAs (39). In *Caulobacter crescentus*, subcellular localization of mRNA degradation proteins may affect global mRNA stability (40, 41). Furthermore, in some actinomycetes, PNPase might be regulated by the stringent response alarmones guanosine-3'-diphosphate-5'-triphosphate (pppGpp) and/or guanosine-3',5'-bisphosphate (ppGpp), collectively referred to as (p)ppGpp (42, 43). Many bacteria synthesize (p)ppGpp in response to energy stress (44–47), in which it generally facilitates adaptation by upregulating stress-associated genes and downregulating those associated with growth (46, 48–52). (p)ppGpp was reported to inhibit the activity of PNPase in two actinomycetes, *Streptomyces coelicolor* and *Nonomuraea* (42, 43), suggesting that the stringent response may directly stabilize mRNA as part of a broader response to energy starvation.

Another explanation for stress-induced transcript stabilization may be that reduced transcript abundance directly leads to increased transcript stability. mRNA abundance and half-life were reported to be inversely correlated in multiple bacteria, including *M.*

tuberculosis (3, 8, 53, 54), and mRNA abundance is lower on a per-cell basis for most transcripts in nongrowing bacteria. Nevertheless, the causal relationships between translation, mRNA abundance, RNase expression, and mRNA stability in nongrowing bacteria remain largely untested.

Given the importance of adaptation to energy starvation for mycobacteria, we sought to investigate the mechanisms by which mRNA stability is globally regulated. Here, we show that the global mRNA stabilization response occurs also in *Mycobacterium smegmatis*—a nonpathogenic model commonly used to study the basic biology of mycobacteria — under hypoxia and carbon starvation. Remarkably, we found that hypoxia-induced mRNA stability is rapidly reversible, with reaeration causing immediate mRNA destabilization even in the absence of protein synthesis. As expected, transcript levels from hypoxic cells were lower on a per-cell basis than those from aerated cultures. However, our data are inconsistent with a model in which mRNA abundance dictates the degradation rate, as has been shown for log-phase *E. coli* (53) and *Lactococcus lactis* (54). Instead, our findings support the idea that mRNA stability is rapidly tuned in response to alterations in energy metabolism. This effect does not require the stringent response or changes in abundance of RNA degradation proteins and can be decoupled from growth status.

RESULTS

mRNA is stabilized as a response to carbon starvation and hypoxic stress in *Mycobacterium smegmatis*. The mRNA pools of *E. coli* and other well-studied bacteria were reported to be globally stabilized during conditions of stress, resulting in increased mRNA half-lives (3–13). Rustad et al. reported a similar phenomenon in *M. tuberculosis* under hypoxia and cold shock (3). We sought to establish *M. smegmatis* as a model for study of the mechanistic basis of mRNA stabilization in mycobacteria under stress conditions. We therefore subjected *M. smegmatis* to hypoxia and carbon starvation and measured mRNA half-lives for a subset of genes by blocking transcription with rifampin (RIF) and measuring mRNA abundance at multiple time points using quantitative PCR (qPCR). We used a variation of the Wayne and Hayes model (55) to produce a gradual transition from aerated growth to hypoxia-induced growth arrest by sealing cultures in vials with defined headspace ratios and allowing them to slowly deplete the available oxygen (Fig. 1A and B). We tested a set of mRNAs that included transcripts with and without leaders, monocistronic and polycistronic transcripts, and transcripts with both relatively short and relatively long half-lives in log phase. We observed that all of the analyzed transcripts had increased half-lives under hypoxia compared to those of log-phase normoxic cultures, and similarly, transcripts were more stable under carbon starvation than in rich media (Fig. 1C and D). Thus, *M. smegmatis* appears to be a suitable model for investigating the mechanisms of stress-induced mRNA stabilization in mycobacteria. To ensure that the apparent mRNA stabilization was not an artifact of reduced RIF activity in nongrowing cells, we confirmed that RIF indeed blocked transcription in hypoxia-arrested *M. smegmatis* (Fig. 1E). We noted that transcripts became progressively more stable as oxygen levels dropped and growth ceased; 40 h after sealing the vials, mRNA half-lives were too long to be reliably measured by our methodology. We sought to focus our studies on the mechanisms that underlie the initial mRNA stabilization process during the transition into hypoxia-induced growth arrest. We therefore conducted most of our subsequent experiments 18 to 24 h after sealing the vials, when growth had nearly ceased and transcripts were 9-fold to 25-fold more stable than during log phase. We refer to these conditions as 18-h hypoxia and 24-h hypoxia.

(p)ppGpp does not contribute to mRNA stabilization under hypoxia or carbon starvation. Given recent reports that (p)ppGpp may directly inhibit the enzymatic activity of the exoribonuclease PNPase (42, 43), we wondered whether mRNA stabilization as observed under carbon starvation and hypoxia is regulated by (p)ppGpp in mycobacteria. We obtained a double mutant strain of *M. smegmatis* (56) that lacks both genes implicated in the production of (p)ppGpp (Δ*rel* Δ*sas2*) and compared the mRNA
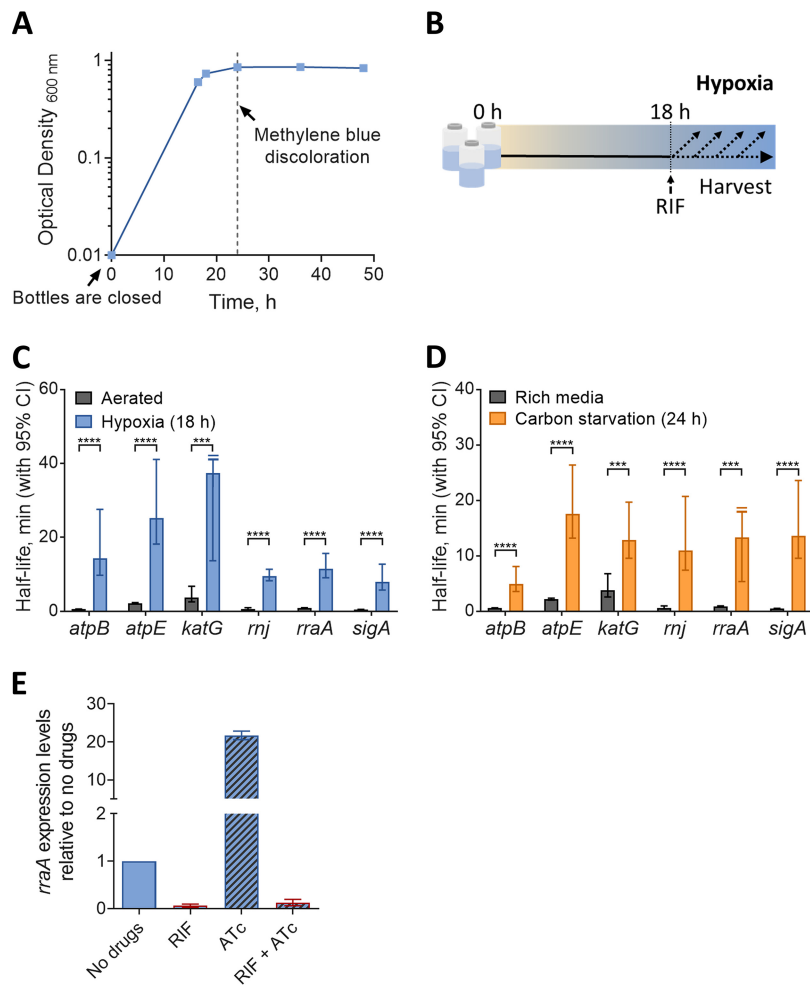
FIG 1 Transcript half-lives are increased in response to hypoxia and carbon starvation stress. (A) Growth kinetics for *M. smegmatis* under hypoxia using a variation of the Wayne and Hayes model (55), showing OD stabilization at 18 to 24 h. Oxygen depletion was assessed qualitatively by methylene blue discoloration. (B) *M. smegmatis* was sealed in vials to produce a hypoxic environment, and at 18 h, transcription was inhibited with RIF and samples were collected thereafter. Transcript half-lives for the indicated genes were measured for *M. smegmatis* mc²155 after blocking transcription with 150 µg/ml RIF. (C and D) RNA samples were collected during log-phase normoxia and hypoxia (18 h after closing the bottles) (C) or during log phase in 7H9 supplemented with ADC, glycerol, and Tween 80 (rich medium) or 7H9 with Tyloxapol only (carbon starvation, 24 h) (D). mRNA degradation rates were compared using linear regression ($n = 3$), and half-lives were determined by the negative reciprocal of the best-fit slope. Error bars are 95% confidence intervals (CI). ***, $P < 0.001$; ****, $P < 0.0001$. When a slope of zero was included in the 95% CI (indicating no degradation), the upper limit for half-life was unbounded, indicated by a clipped error bar with a double line. (E) RIF blocks overexpression of an ATc-inducible gene (*rraA*) in hypoxic cultures. Forty hours after the bottles were sealed, cultures were treated with 50 ng/ml ATc and/or 150 µg/ml RIF or the drug vehicle (DMSO) for 1 h. Expression levels (qPCR) are displayed relative to those with no drugs (DMSO treatment). ATc, RIF, and DMSO solutions were degassed prior to addition. Error bars are standard deviations (SD).

half-lives of a subset of genes to those of wild-type mc²155 under hypoxia, log-phase normoxia, and carbon starvation. The Δ*rel* Δ*sas2* strain had a growth defect during adaptation to hypoxia and carbon starvation (Fig. 2A and C), as predicted (57). However, we found no significant decrease in mRNA stabilization in the mutant strain (Fig. 2B and D), indicating that the mRNA stabilization observed under hypoxia and carbon starvation is independent from the stringent response. Interestingly, the mutant strain displayed increased mRNA stabilization for a few transcripts under carbon starvation conditions, which may be an indirect consequence of altered transcription rates (see Discussion).
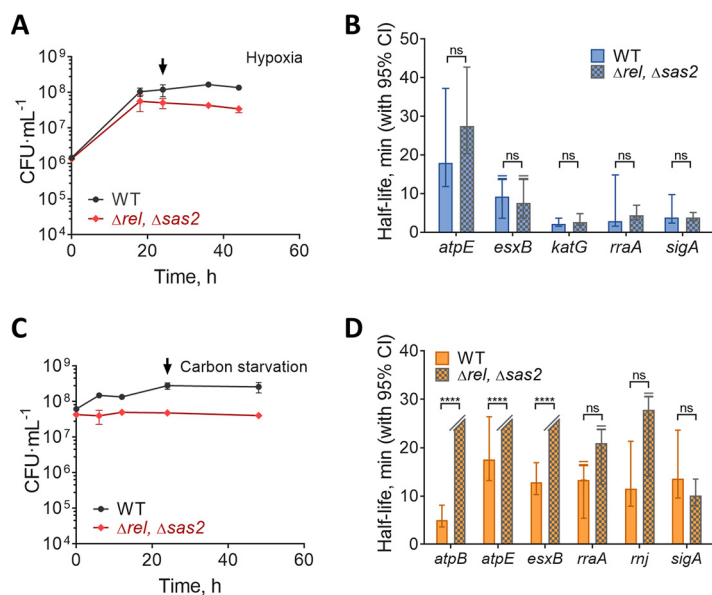
FIG 2 Transcript stabilization in hypoxia and carbon starvation are not dependent on the stringent response. (A) Growth kinetics for *M. smegmatis* mc²155 (wild type [WT]) and Δ*rel* Δ*sas2* strains cultured in 7H9 in flasks sealed at time zero. (B) Transcript half-lives for a set of genes 24 h after sealing of the hypoxia bottles (arrow in panel A). RNA samples were collected after transcription was blocked with 150 μg/ml RIF (degassed). (C) Bacteria were grown to log phase in 7H9 supplemented with ADC, glycerol, and Tween 80 and then transferred to 7H9 supplemented with only Tyloxapol at time zero. (D) Transcript stability for a set of genes 22 h after transfer to carbon starvation medium (arrow in panel C). (A and C) The means and SD of triplicate cultures are shown. (B and D) Half-lives were compared using linear regression analysis (*n* = 3). Error bars are 95% CI. ****, *P* < 0.0001; ns, not significant (*P* > 0.05). In cases where no degradation was observed or when the upper 95% CI limit was unbounded, the bar or upper error bar were clipped, respectively.

Hypoxia-induced mRNA stability is reversible and independent of mRNA abundance. We wondered if the observed stress-induced transcript stabilization could be reversed by restoration of a favorable growth environment. To test this, we prepared 18-h hypoxia cultures, opened the vials, and agitated them for 2 min to reexpose the bacteria to oxygen before blocking transcription with RIF and sampling thereafter (Fig. 3A, top). We found that, for all transcripts tested, half-lives were significantly decreased compared to those observed under hypoxia and similar to those observed in log phase (Fig. 3B). While the mechanisms of stress-induced mRNA stabilization are largely unknown, multiple studies have reported inverse correlations between mRNA abundance and half-life in bacteria (3, 8, 53, 54). mRNA abundance was decreased for most transcripts tested in hypoxia-adapted *M. smegmatis*. We therefore considered the possibility that the dramatic increase in mRNA degradation upon reexposure to oxygen was triggered by a burst of transcription. Indeed, we found increased expression levels for four of five genes tested after 2 min of reaeration, showing that transcription is rapidly induced upon return to a favorable environment (Fig. 3C). To test the idea that mRNA is destabilized by reaeration as a consequence of a transcriptional burst and/or increased mRNA abundance, we modified our reaeration experiment by blocking transcription with RIF 1 min prior to reaeration (Fig. 3A, bottom). Surprisingly, every transcript tested was destabilized by reaeration despite the absence of new transcription. For most transcripts, the reaeration half-lives were indistinguishable, regardless of whether RIF was added prior to opening the vials or 2 min after (Fig. 3B). Our results therefore do not support the idea that changes in mRNA abundance alone can explain the mRNA stabilization and destabilization observed in response to changes in energy status.

We wanted to further explore whether mRNA abundance alone could influence transcript degradation. We obtained a strain bearing *dCas9* and a nonspecific sgRNA under the control of an anhydrotetracycline (ATc)-inducible promoter (58) and com-
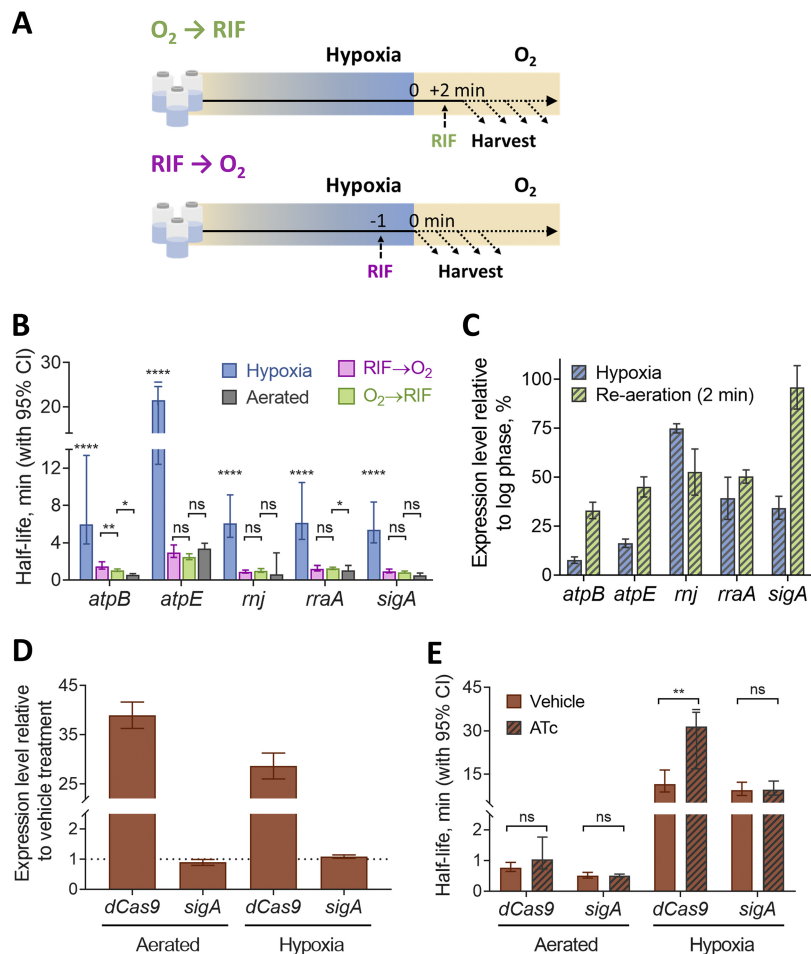
FIG 3 Hypoxia-induced mRNA stability is reversible and independent of mRNA abundance. (A) *M. smegmatis* was sealed in vials for 18 h to produce a hypoxic environment and then reexposed to oxygen for 2 min before transcription was inhibited with RIF (top) or injected with RIF 1 min prior to opening of the vials and reexposing them to oxygen (bottom). (B) Transcript half-lives for a set of genes are displayed for log-phase normoxia cultures, hypoxia (18 h), and reaeration with RIF added either before or after opening of the vials. Half-lives were compared by linear regression analysis ($n = 3$). (C) Expression levels of transcripts under hypoxia (18 h) or with a 2-min reaeration relative to the expression levels in log-phase normoxia cultures (percentages). Error bars are SD. (D) Expression levels of transcripts under hypoxia (18 h) or log-phase normoxia after being treated with 200 ng/ml ATc for 1 h or 10 min, respectively, to induce *dCas9* overexpression, relative to the expression levels in cultures treated with an H_2O vehicle (percentages). Error bars are SD. (E) Transcript half-lives for *dCas9* and *sigA* for log-phase normoxia and hypoxia (18 h) after induction of *dCas9* with ATc or after vehicle treatment as shown in panel D. (B and E) Degradation rates were compared using linear regression ($n = 3$), and half-lives were determined by the negative reciprocal of the best-fit slope. Error bars are 95% CI. *, $P < 0.05$; **, $P < 0.01$; ****, $P < 0.0001$; ns, $P > 0.05$. RIF added to hypoxic cultures was degassed prior to its addition.

pared the *dCas9* transcript stability under hypoxia and normoxia after ATc induction or at basal levels. We found that despite a 34-fold transcript upregulation following ATc induction, the half-life of *dCas9* mRNA was not significantly different from that of the uninduced control in log phase. Under hypoxia, its 28-fold upregulation was associated with an increase in *dCas9* mRNA half-life compared to in the no-drug control (Fig. 3D and E). Together, our results show that increased mRNA abundance does not necessarily result in a faster decay rate.

mRNA stability is modulated independently of RNase protein levels. Another potential explanation for increased mRNA degradation after reaeration is the upregulation of mRNA degradation proteins, such as RNase E. To assess the role of a sudden burst in protein levels, we used two approaches. First, we constructed strains encoding FLAG-tagged RNase E, cMyc-tagged PNPase, or cMyc-tagged msmeg_1930 (predicted
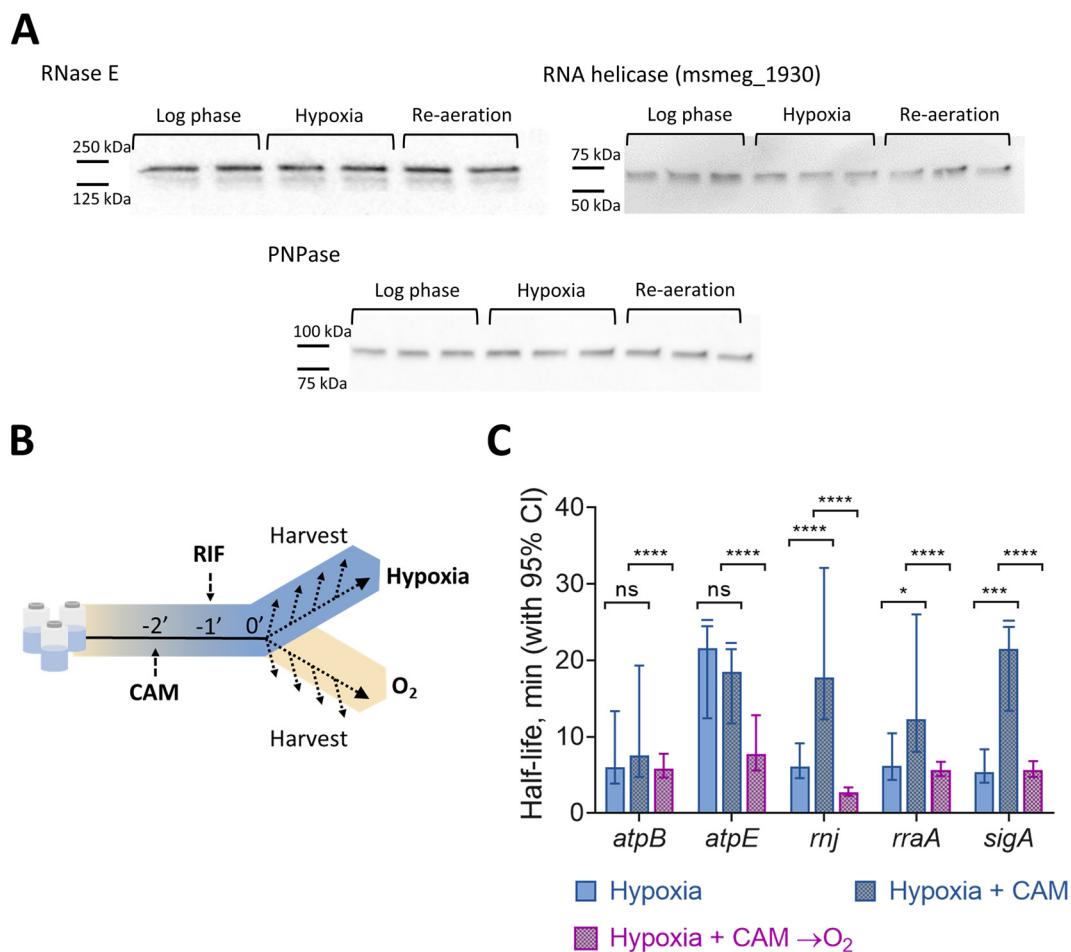
A

RNase E

RNA helicase (msmeg_1930)

PNPase

B

C

FIG 4 mRNA stability is regulated independently of degradation protein levels. (A) Western blotting for FLAG-tagged RNase E and cMyc-tagged PNPase or RNA helicase (msmeg_1930) in *M. smegmatis* under log-phase normoxia and hypoxia (18 h) and with a 2-min reaeration. Samples were normalized to the total protein level, and levels were similar on a per-OD basis under all conditions. (B) Translation was inhibited in hypoxic cultures by 150 μg/ml CAM 1 min before the addition of 150 μg/ml RIF. RNA was harvested at time points beginning 2 min after the addition of CAM. (C) Transcript half-lives for samples from hypoxic cultures with the drug vehicle (ethanol), for hypoxic cultures after translation inhibition, and for cultures with 2 min of reaeration after translation inhibition. Degradation rates were compared using linear regression ($n = 3$), and half-lives were determined by the negative reciprocal of the best-fit slope. Error bars are 95% CI. ns, $P > 0.05$; *, $P < 0.05$; ***, $P < 0.001$; ****, $P < 0.0001$. Drugs and drug vehicles added to the hypoxic cultures were degassed prior to their addition.

RNA helicase). We determined protein levels by Western blotting in log phase, with 18 h of hypoxia, and after 18 h of hypoxia followed by 2 min of reaeration. Levels of all three of these predicted RNA degradation proteins remained unchanged under the three conditions (Fig. 4A).

Because we do not know all of the proteins that contribute to mRNA degradation in mycobacteria, our second approach was to test the global importance of translation in reaeration-induced mRNA destabilization. We blocked translation with chloramphenicol (CAM) in 18-h hypoxia cultures and then added RIF. Samples were collected for cultures that remained under hypoxia as well as those that were reaerated for 2 min (Fig. 4B). For three of the five genes tested, we found that CAM caused increased mRNA stability under hypoxia. This is consistent with CAM's mechanism of action and published work (59–61). CAM inhibits elongation by preventing peptidyl transfer (62–64) and causing ribosomal stalling (65). Global stabilization of mRNA pools has been reported when elongation inhibitors, but not initiation inhibitors, are used for example in log-phase cultures of *E. coli* (65) or in *Saccharomyces cerevisiae* (66). We hypothesize that stalled ribosomes may increase mRNA stability by masking RNase cleavage sites. However, despite the stabilization caused by CAM itself, we observed mRNA destabi-
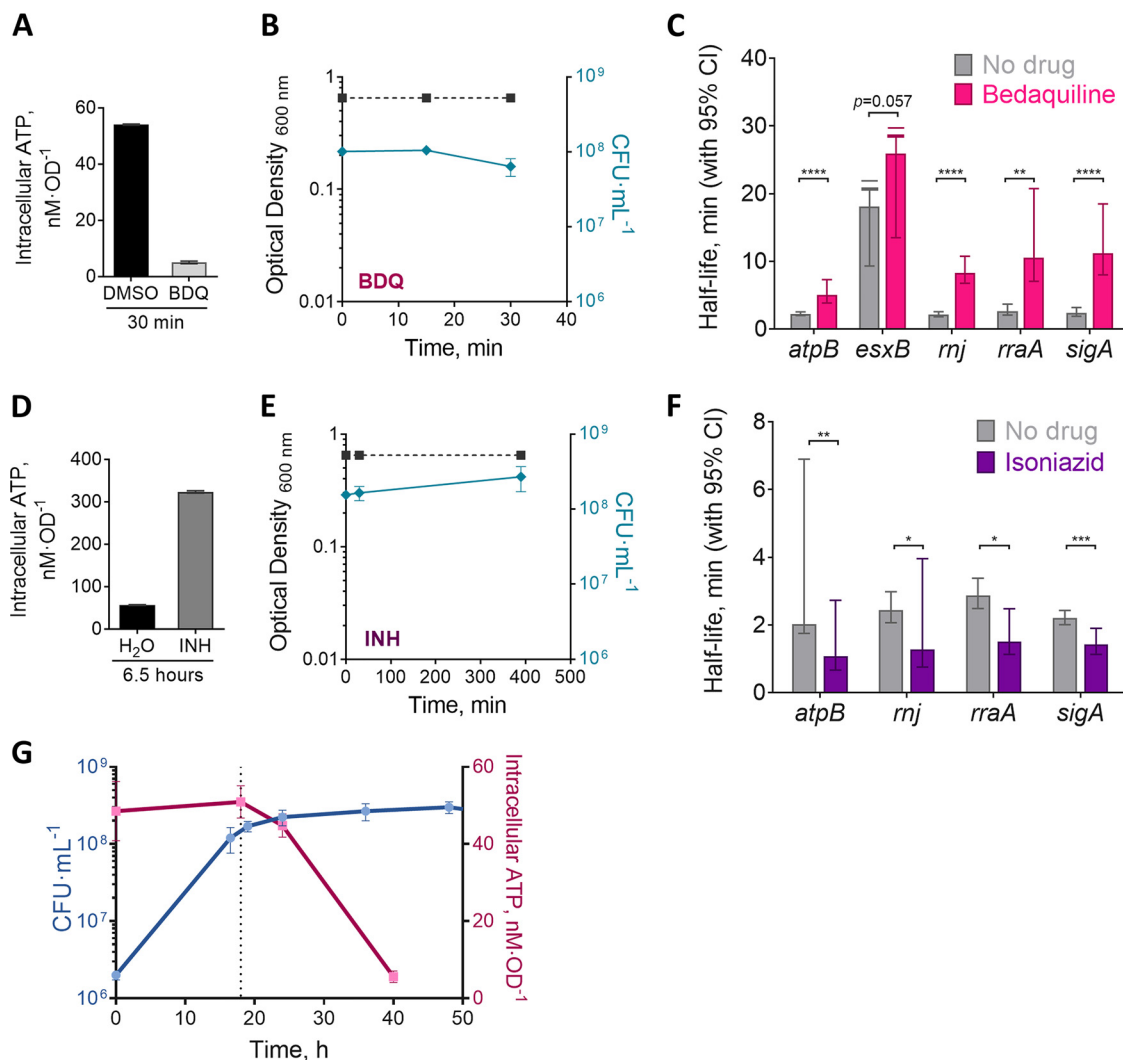
FIG 5 mRNA stability is modulated in response to changes in metabolic status. (A) *M. smegmatis* was cultured in MMA media for 22 h to OD$_{600}$ 0.8 before being treated with 5 μg/ml BDQ or the vehicle (DMSO) for 30 min. Intracellular ATP was determined using the BacTiter-Glo kit. (B) Growth kinetics for *M. smegmatis* from panel A in the presence of BDQ. (C) Transcript half-lives for a subset of transcripts collected during intracellular ATP depletion (30 min with BDQ) or at the basal levels (30 min with DMSO). (D) As in panel A, but for *M. smegmatis* treated with 500 μg/ml INH or the vehicle (H$_2$O) for 6.5 h. (E) Growth kinetics for *M. smegmatis* from panel D in the presence of INH. (F) Transcript half-lives for a subset of transcripts after 6.5 h of INH or vehicle treatment. (G) Growth kinetics for *M. smegmatis* transitioning into hypoxia, and intracellular ATP levels at different stages. Bottles were sealed at time zero. The dotted line represents the time at which transcript stability analyses were made for the hypoxia (18 h) condition for Fig. 1, 3, and 4. In C and F, half-lives were compared using linear regression analysis (*n* = 3). Error bars are 95% CI. *, *P* < 0.05; **, *P* < 0.01; ***, *P* < 0.001; ****, *P* < 0.0001. ATP was measured in biological triplicate cultures and is representative of at least two independent experiments.

lization in response to reaeration (Fig. 4C). These results suggest that reaeration-induced destabilization does not require synthesis of new RNA degradation proteins. Taken together, our data suggest that tuning of protein levels is not the primary explanation for mRNA stabilization during early adaptation to hypoxia.

mRNA stability is modulated in response to changes in metabolic status. The rapidity of mRNA destabilization following reaeration suggested that mRNA degradation is tightly regulated in response to changes in energy metabolism. We tested this hypothesis by treating log-phase cultures with 5 μg/ml bedaquiline (BDQ), a potent inhibitor of the ATP synthase F$_o$F$_1$ (67). We used minimal medium that contained acetate as the only carbon source (minimal medium acetate [MMA]) in order to make the respiratory chain the sole source of ATP synthesis. After 30 min of exposure, intracellular ATP levels were reduced by more than 90% compared to levels in cells treated with vehicle (dimethyl sulfoxide [DMSO]), without affecting viability (Fig. 5A and

B). We then measured half-lives for a set of transcripts under these conditions. mRNA half-lives were dramatically increased in BDQ-treated cells for most of the genes that we tested (Fig. 5C), indicating that mRNA degradation rates are rapidly altered in response to changes in energy metabolism status.

We then wondered if we could increase mRNA degradation rates by increasing intracellular ATP levels. To test this, we treated *M. smegmatis* cultures with isoniazid (INH), a prodrug that interferes with the synthesis of mycolic acids and also leads to an accumulation of intracellular ATP due to increased oxidative phosphorylation (68). We exposed *M. smegmatis* to 500 μg/ml INH for 6.5 h to confirm that we had achieved bacteriostasis (the *M. smegmatis* doubling time in MMA medium is ~6 h). As shown in Fig. 5D, INH caused a dramatic increase in intracellular ATP after 6.5 h without affecting cell viability (Fig. 5E). Remarkably, mRNA half-lives were significantly decreased in response to INH (Fig. 5F). To our knowledge, this is the first report of bacterial mRNA being destabilized rather than stabilized in response to a growth-impairing stressor. Our results indicate that mRNA stability is regulated not in response to growth status *per se* but rather to energy metabolism. Although we interpreted ATP levels as a reflection of metabolic status in our INH and BDQ assays, the coupling between mRNA degradation and metabolic status does not appear to be mediated by ATP directly. We measured ATP levels in cultures during the transition to hypoxia-induced growth arrest and found that although ATP levels ultimately decrease under hypoxia as has been reported elsewhere (69, 70), mRNA stabilization precedes the drop in ATP levels (Fig. 5G).

DISCUSSION

Stressors that cause bacteria to slow or stop growth are typically associated with increased mRNA stability (3–9, 11–13). Many of these same stressors reduce energy availability (69, 70), requiring reductions in energy consumption and optimization of resource allocation. We speculate that the decreased mRNA turnover that accompanies such conditions may be an energy conservation mechanism. For *M. tuberculosis*, hypoxia can lead to generation of bacterial subpopulations with various degrees of antibiotic tolerance (71–73), facilitating bacterial survival and the acquisition of drug resistance-conferring mutations. Understanding the mechanisms that support the transitions into nongrowing states and subsequent survival in these states is therefore a priority.

The transcriptome of *M. tuberculosis* has been shown to be stabilized under cold shock and hypoxia (3). Here, we found that *M. smegmatis* also dramatically stabilized its mRNA in response to carbon starvation and hypoxia. For the first time, to our knowledge, we tested the speed at which this stabilization is reversed in mycobacteria upon restoration of energy availability. Remarkably, mRNAs are rapidly destabilized within minutes of reaeration of hypoxic cultures, suggesting that tuning of mRNA degradation rates is an early step in the response to changing energy availability.

The most straightforward explanation for stress-induced mRNA stabilization seems to be downregulation of the mRNA degradation machinery. Indeed, RNase E is downregulated at the transcript level under hypoxia, and abundance of cleaved RNAs is reduced (74). However, we found that protein levels were unchanged for RNase E and two other proteins predicted to be core components of the mRNA degradation machinery. This is largely consistent with what was reported for *M. tuberculosis* in a quantitative proteomics study (37), although in that case there was an apparent reduction in levels of an RNA helicase. To address this question in a more agnostic fashion, we tested the importance of translation for transcript destabilization upon reexposure of hypoxic cultures to oxygen. However, reaeration triggered increased transcript degradation even in the absence of new protein synthesis. Regulation of degradation protein levels therefore does not appear to contribute to mRNA stabilization during the initial response to energy stress. However, we found that upon longer periods of hypoxia, transcripts were stabilized to a greater extent than what we observed 18 h after sealing the vials. This suggests that mRNA stabilization progres-

sively increases and may involve multiple mechanisms. As this work focused on the initial transition into hypoxia-induced growth arrest, we cannot discount the possibility that downregulation of the RNA degradation machinery is important for further mRNA stabilization in later hypoxia stages.

Interestingly, we found greater mRNA stabilization in hypoxic cultures treated with CAM. This may result from stalled ribosomes (62, 64) masking RNase cleavage sites. Furthermore, the burst of transcription upon reaeration is blocked by the presence of CAM, causing up to a 4-fold decrease in transcript abundance in the CAM-treated cultures compared to that in the vehicle-treated cultures. This is consistent with the idea that transcription and translation are physically coupled, and blocking translation therefore prevents RNA polymerase from efficiently carrying out transcript elongation, as was reported for *E. coli* (75–79). The results obtained from the Δ*rel* Δ*sas2* strain are also consistent with the idea that the presence of ribosomes affects mRNA stability. Under carbon starvation, this strain had rRNA levels 3-fold higher than those of the WT strain, consistent with the known role of (p)ppGpp in downregulating ribosome biogenesis (80–82). Interestingly, some transcripts were hyperstabilized in the Δ*rel* Δ*sas2* strain under carbon starvation, showing virtually no degradation (Fig. 2D). We speculate that the observed mRNA hyperstabilization is caused by increased ribosome abundance, resulting in augmented mRNA-ribosome associations that ultimately protect transcripts from RNases. Alternatively, the increased abundance of rRNA may protect mRNA indirectly by providing alternative targets that compete for interaction with RNases (65).

Transcript abundance has been found to be inversely correlated with mRNA stability in exponentially growing bacteria (3, 8, 53, 54, 83), and experimental manipulation of transcription rates of subsets of genes affected their degradation rates (3, 54). Together, these studies suggest that high rates of transcription inherently increase degradation rates. We report here that during oxygen depletion, transcript levels are reduced in *M. smegmatis*, which led us to ask whether increased transcript half-lives under stress are a direct result of reduced mRNA levels. However, our data are inconsistent with this idea; mRNA is rapidly destabilized upon reaeration even in the absence of new transcription. We note that one study reported a weak positive correlation between mRNA abundance and stability in log-phase *E. coli* (12), while another reported mRNA abundance to be positively correlated with stability in carbon-starved *Lactococcus lactis* (8). Together, these observations and our own suggest that the relationship between mRNA stability and abundance is not yet fully understood and may be fundamentally different in growth-arrested bacteria.

The rapid reversibility of hypoxia-induced mRNA stabilization suggests that mRNA decay and energy metabolic status are closely linked. Consistently with this, we have shown that drug-induced energy stress causes mRNA stabilization but that mRNA decay is increased by a drug that induces a hyperactive metabolic state. To our knowledge, this is the first demonstration that the rate of bacterial mRNA degradation can be decoupled from growth rate and suggests that mRNA decay is controlled by energy status rather than growth rate *per se*. The mechanism by which energy status and mRNA decay are coupled remains elusive; the stringent response is not required, and the stabilization of mRNA during adaptation to hypoxia precedes a decrease in ATP levels. Our data are consistent with two general (nonexclusive) models: mRNA decay may be regulated (i) by protection of transcripts from RNase attack and/or (ii) by direct regulation of the activities of the RNases. Possible explanations that fall within one or both of these frameworks include changes in ribosome occupancy, the presence of other RNA-binding proteins, regulation of the subcellular localization of mRNAs and/or the RNA degradation machinery, and altered degradosome composition. These possibilities should be investigated in future work.

MATERIALS AND METHODS

Strains and culture conditions. *Mycobacterium smegmatis* strain mc²155 or its derivatives (Table 1) were grown in rich medium, Middlebrook 7H9 with albumin dextrose catalase (ADC; final concentrations,

TABLE 1 Strains used and sources

Strain	Characteristics	Reference or source
mc²155	*M. smegmatis*, wild type	85
SS-M_0072	mc²155 derivative transformed with plasmid pSS162, containing an ATc-inducible copy of *rraA*	This work
SS-M_0296	mc²155 in which the native copy of RNase E (*rne*) is N-terminally tagged with the 6×His-3×FLAG-TEV-4×Gly linker (CACCACCACCACCACCACGATT ACAAGGATCACGATGGCGATTACAAGGATC ATGACATCGACTATAAGGACGATGACGATA AGGAGAACCTGTACTTCCAGGGCGGCGGCGGC)	This work
SS-M_0412	SS-M_0296 derivative containing a second copy of PNPase (msmeg_2656) with its predicted native promoter and 5′ UTR and N-terminally tagged with the cMyc-4×Gly linker (GAGCAGAAGCTGATC TCGGAAGAGGACCTCGGCGGCGGCGGC) contained within the Giles-integrating plasmid pSS282 (Hyg^r)	This work
SS-M_0416	SS-M_0296 derivative containing a second copy of the RNA helicase (msmeg_1930) with its predicted native promoter and 5′ UTR and C-terminally tagged with the 4×Gly linker-cMyc (GGCGGCGGCGG CGAGCAGAAGCTGATCTCGGA) contained within a Giles-integrating plasmid pSS285 (Hyg^r)	This work
Δ*rel*_Msm strain	mc²155 derivative, Δ*rel* Δ*sas2*	56
SS-M_0203	mc²155 derivative transformed with plasmid pJR962, containing an ATc regulated *dCas9*	58

5 g/liter bovine serum albumin fraction V [BSA], 2 g/liter dextrose, 0.85 g/liter NaCl, and 3 mg/liter catalase), 0.2% glycerol, and 0.05% Tween 80, which was shaken at 200 rpm and 37°C to an optical density at 600 nm (OD$_{600}$) of ~0.8, unless specified otherwise. For hypoxic cultures, we modified the Wayne and Hayes model (55). Bacteria were cultured in 30.5- by 58-mm serum bottles (Wheaton; item 223687, 20 ml) using rich medium and an initial OD$_{600}$ of 0.01. Bottles were sealed with a vial crimper (Wheaton; item W225303) using rubber stoppers (Wheaton; item W224100-181) and aluminum seals (Wheaton; item 224193-01). Oxygen levels were qualitatively monitored using methylene blue.

For carbon starvation cultures, cells were grown to log phase (OD$_{600}$ = 0.8) in rich medium, pelleted, and rinsed three times with carbon starvation medium (Middlebrook 7H9 with 5 g/liter BSA, 0.85 g/liter NaCl, 3 mg/liter catalase, and 0.05% Tyloxapol) at 4°C and then resuspended in carbon starvation medium to an OD$_{600}$ of 0.8 and incubated at 200 rpm and 37°C.

The RNase E-tagged strain (SS-M_0296) was built using a two-step process. Plasmid pSS250 was derived from pJM1 (84) and contained 1 kb of the sequence upstream and downstream of the *rne* (msmeg_4626) start codon, with the sequence encoding 6×His-3×FLAG-TEV-4×Gly inserted after the start codon. Constructs were built using NEBuilder HiFi (E2621). Integrants were selected with 200 μg/ml hygromycin and confirmed by sequencing. Counterselection with 15% sucrose was followed by PCR screening to identify isolates that underwent second crossovers resulting in loss of the plasmid and retention of tagged *rne*.

The PNPase-tagged strain (SS-M_0412) was built by inserting a second copy of *pnp* (msmeg_2656) with an N-terminal cMyc-4×Gly construct and its predicted native promoter and 5′ untranslated region (UTR) at the Giles phage integration site (plasmid pSS282) into strain SS-M_0296. The RNA helicase-tagged strain (SS-M_0416) was constructed in a similar way but with a C-terminal 4×Gly-cMyc tag on msmeg_1930 (plasmid pSS285).

RNA extraction and determination of mRNA stability. Biological triplicate cultures were treated with rifampin (RIF) to a final concentration of 150 μg/ml to halt transcription, and RNA was extracted at various time points thereafter. For exponential and carbon starvation cultures, 7 ml was collected per replicate and time point and snap-frozen in liquid nitrogen (LN2). For hypoxic samples, degassed RIF was injected using a 30-gauge needle, and all samples were sacrificially collected per time point and replicate (7 ml) and snap-frozen in LN2 within 6 s of unsealing.

Samples were stored at −80°C and thawed on ice immediately before RNA extraction. Cells were pelleted at 4°C, resuspended in 1 ml TRIzol (Invitrogen), transferred to 2-ml disruption tubes (OPS Diagnostics; 100-μm zirconium lysing matrix, molecular grade), and lysed using a FastPrep-24 5G instrument (MP Biomedical) (3 cycles of 7 m/s for 30 s, with 2 min on ice between cycles). Chloroform (300 μl) was added, samples were centrifuged for 15 min at 21,130 × *g* and 4°C, and RNA was recovered from the aqueous layer and purified with a Direct-zol RNA miniprep kit according to the manufacturer's instructions with an in-column DNase treatment. Agarose gels were used to verify RNA integrity.

For cDNA synthesis, 600 ng of total RNA was mixed with 0.83 μl 100 mM Tris, pH 7.5, and 0.17 μl 3-mg/ml random primers (NEB) in 5.25 μl, denatured at 70°C for 10 min, and snap-cooled. Reverse transcription was performed for 5 h at 42°C using 100 U ProtoScript II reverse transcriptase (NEB), 10 U

TABLE 2 Primers for qPCR

Primer name (reference)	Gene (locus tag)	Directionality	Sequence (5′→3′)
SSS903	atpB (msmeg_4942)	Forward	TGTTCGTGTTCGTCTGCTAC
SSS904	atpB (msmeg_4942)	Reverse	CGGCTTGGCGAGTTCTT
SSS909	atpE (msmeg_4941)	Forward	GGGTAACGCGCTGATCTC
SSS910	atpE (msmeg_4941)	Reverse	GAAGGCCAGGTTGATGAAGTA
SSS1241	dCas9	Forward	GACAAGTCGAAGTTCCTGATGTA
SSS1242	dCas9	Reverse	GATCTGCTTGTTCGGGTAGTT
SSS537	esxB (msmeg_0065)	Forward	GGTGAGGACACAGGGAAATAAG
SSS538	esxB (msmeg_0065)	Reverse	CGGAGATGCGCTCGAAAT
SSS856	katG (msmeg_6384)	Forward	GGCCCAATCAGCTCAATCT
SSS857	katG (msmeg_6384)	Reverse	CGGACCGGTAGTCGAAATC
SSS706	rnj (msmeg_2685)	Forward	TCATCCTCTCATCGGGTTTC
SSS707	rnj (msmeg_2685)	Reverse	TTCGCGCTCAACCTTCT
SSS697	rraA (msmeg_6439)	Forward	AACTACGGCGGCAAGAT
SSS698	rraA (msmeg_6439)	Reverse	GTCGAGAGGATCGACTTCAG
JR273 (58)	sigA (msmeg_2758)	Forward	GACTACACCAAGGGCTACAAG
JR274 (58)	sigA (msmeg_2758)	Reverse	TTGATCACCTCGACCATGTG

RNase inhibitor (murine; NEB), a mix containing 0.5 mM each deoxynucleoside triphosphate (dNTP), and 5 mM dithiothreitol (DTT) in a final volume of 10 μl. RNA was degraded with 5 μl each 0.5 mM EDTA and 1 N NaOH at 65°C for 15 min, followed by 12.5 μl of 1 M Tris-HCl, pH 7.5. cDNA was purified using the MinElute PCR purification kit (Qiagen) according to the manufacturer's instructions. mRNA abundance (A) over time (t) was determined for different genes (primers in Table 2) by quantitative PCR (qPCR) using iTaq SYBR green (Bio-Rad) with 400 pg of cDNA and 0.25 μM each primer in 10-μl reaction mixtures, with 40 cycles of 15 s at 95°C and 1 min at 61°C (Applied Biosystems 7500). Abundance was expressed as the negative threshold cycle ($-C_T$) [reflecting the $\log_2 A(t)$]. Linear regression was performed on $-C_T$ values versus time where the negative reciprocal of the best-fit slope estimates mRNA half-life (see Text S1 and Fig. S1 in the supplemental material). In many cases, the decay curves were biphasic, with a rapid period of decay followed by a period of slow or undetectable decay. In these cases, only the initial, steeper slope was used for calculation of half-lives.

mRNA stability during reaeration and translational inhibition. Translation was halted by 150 μg/ml chloramphenicol, rifampin was added 1 min later, and samples were collected starting 1 min after that. For reaeration experiments, 18-h hypoxia cultures were opened and the contents transferred to 50-ml conical tubes, and triplicate samples were taken 2, 7, 12, 17, and 32 min after we opened the bottles and snap-frozen in LN2. Rifampin was added either 1 min before (transcription inhibition during hypoxia) or 2 min after (transcription inhibition after reaeration) we opened the bottles.

BDQ and INH treatments. Cultures were grown to an OD_{600} of ~1.0 in rich medium, rinsed twice in minimal medium acetate (MMA) wash (final concentrations, 0.5 g/liter L-asparagine, 1 g/liter KH_2PO_4, 2.5 g/liter Na_2HPO_4, 0.5 g/liter $MgSO_4 \cdot 7H_2O$, 0.5 mg/ml $CaCl_2$, 0.1 mg/ml $ZnSO_4$, 0.1% CH_3COONa, 0.05% tyloxapol, pH 7.5) at 4°C, resuspended in MMA (MMA wash plus 50 mg/liter ferric ammonium citrate) to an OD_{600} of 0.07, and grown for 24 h to an OD_{600} of ~0.8. To remove the extracellular ATP, 30 min before drug treatment, cells were pelleted and rinsed in prewarmed MMA wash, resuspended in prewarmed MMA, and returned to the incubator. Bedaquiline (BDQ), isoniazid (INH), or their vehicles were added to final concentrations of 5 μg/ml (BDQ) or 500 μg/ml (INH). Samples were taken 30 min after the addition of BDQ or 6.5 h after the addition of INH for half-life and ATP determinations.

For half-life measurements, BDQ cultures were sampled 0, 3, 6, 9, 12, 15, and 21 min after addition of RIF, and INH cultures were sampled 0, 4, 8, and 12 min after addition of RIF. RNA extractions were performed as described above, with the following modifications: cell disruption was performed using 2-ml tubes prefilled with lysing matrix B (MP Biomedical) and 3 cycles of 10 m/s for 40 s, RNA was recovered from the aqueous layer by isopropanol precipitation and resuspension in H_2O, and samples were treated with 5 U of Turbo DNase (Ambion) in the presence of 80 U of RNase inhibitor, murine (NEB) for 1 h at 37°C with agitation. RNA was purified with an RNeasy minikit (Qiagen) according to the manufacturer's specifications.

Intracellular ATP estimation. ATP was estimated by BacTiter-Glo (Promega). For BDQ or INH treatments, 1 ml of culture was pelleted at ~21°C for 1 min at 21,130 × g, the supernatant removed, and cells resuspended in 1 ml of prewarmed MMA containing BDQ, INH, or vehicle to match the prior treatment conditions. Immediately after, 20-μl samples were transferred to a white 384-well plate (Greiner bio-one) containing 80 μl of BacTiter-Glo reagent and mixed for 5 min at room temperature. Luminescence was measured in a Victor³ plate reader (PerkinElmer) (intracellular ATP). We included controls for the supernatant collected (extracellular ATP), media plus drug/vehicle (background), and ATP standards for constructing standard curves.

To estimate intracellular ATP in normoxia and hypoxia cultures, 20-μl samples were collected at 37°C and immediately combined with the reagent to measure total ATP (intracellular plus extracellular). From the same cultures, 1-ml samples were syringe filtered (PES; 0.2 μm) and the filtrate was combined with the reagent to measure extracellular ATP. Luminescence was measured as described above. Intracellular

ATP was calculated by subtracting the extracellular ATP values from the total ATP values. Hypoxia samples were sacrificially harvested per time point/replicate and combined with the reagent in <6 s.

SUPPLEMENTAL MATERIAL

Supplemental material for this article may be found at https://doi.org/10.1128/mBio .00957-19.

TEXT S1, DOCX file, 0.02 MB.
FIG S1, TIF file, 2.2 MB.

REFERENCES

1. Via LE, Lin PL, Ray SM, Carrillo J, Allen SS, Eum SY, Taylor K, Klein E, Manjunatha U, Gonzales J, Lee EG, Park SK, Raleigh JA, Cho SN, McMurray DN, Flynn JL, Barry CE, III. 2008. Tuberculous granulomas are hypoxic in guinea pigs, rabbits, and nonhuman primates. Infect Immun 76: 2333–2340. https://doi.org/10.1128/IAI.01515-07.

2. Belton M, Brilha S, Manavaki R, Mauri F, Nijran K, Hong YT, Patel NH, Dembek M, Tezera L, Green J, Moores R, Aigbirhio F, Al-Nahhas A, Fryer TD, Elkington PT, Friedland JS. 2016. Hypoxia and tissue destruction in pulmonary TB. Thorax 71:1145–1153. https://doi.org/10.1136/thoraxjnl -2015-207402.

3. Rustad TR, Minch KJ, Brabant W, Winkler JK, Reiss DJ, Baliga NS, Sherman DR. 2013. Global analysis of mRNA stability in Mycobacterium tuberculosis. Nucleic Acids Res 41:509–517. https://doi.org/10.1093/nar/gks1019.

4. Albertson MH, Nyström T, Kjelleberg S. 1990. Functional mRNA half-lives in the marine Vibrio sp. S14 during starvation and recovery. Microbiology 136:2195–2199. https://doi.org/10.1099/00221287-136-11-2195.

5. Georgellis D, Barlow T, Arvidson S, von Gabain A. 1993. Retarded RNA turnover in Escherichia coli: a means of maintaining gene expression during anaerobiosis. Mol Microbiol 9:375–381. https://doi.org/10.1111/j .1365-2958.1993.tb01698.x.

6. Sakamoto T, Bryant DA. 1997. Temperature-regulated mRNA accumulation and stabilization for fatty acid desaturase genes in the cyanobacterium Synechococcus sp. strain PCC 7002. Mol Microbiol 23:1281–1292. https://doi.org/10.1046/j.1365-2958.1997.3071676.x.

7. Thorne SH, Williams HD. 1997. Adaptation to nutrient starvation in Rhizobium leguminosarum bv. phaseoli: analysis of survival, stress resistance, and changes in macromolecular synthesis during entry to and exit from stationary phase. J Bacteriol 179:6894–6901. https://doi.org/10 .1128/jb.179.22.6894-6901.1997.

8. Redon E, Loubiere P, Cocaign-Bousquet M. 2005. Role of mRNA stability during genome-wide adaptation of Lactococcus lactis to carbon starvation. J Biol Chem 280:36380–36385. https://doi.org/10.1074/jbc .M506006200.

9. Anderson KL, Roberts C, Disz T, Vonstein V, Hwang K, Overbeek R, Olson PD, Projan SJ, Dunman PM. 2006. Characterization of the Staphylococcus aureus heat shock, cold shock, stringent, and SOS responses and their effects on log-phase mRNA turnover. J Bacteriol 188:6739–6756. https:// doi.org/10.1128/JB.00609-06.

10. Dressaire C, Picard F, Redon E, Loubiere P, Queinnec I, Girbal L, Cocaign-Bousquet M. 2013. Role of mRNA stability during bacterial adaptation. PLoS One 8:e59059. https://doi.org/10.1371/journal.pone.0059059.

11. Esquerre T, Laguerre S, Turlan C, Carpousis AJ, Girbal L, Cocaign-Bousquet M. 2014. Dual role of transcription and transcript stability in the regulation of gene expression in Escherichia coli cells cultured on glucose at different growth rates. Nucleic Acids Res 42:2460–2472. https://doi.org/10.1093/nar/gkt1150.

12. Chen H, Shiroguchi K, Ge H, Xie XS. 2015. Genome-wide study of mRNA degradation and transcript elongation in Escherichia coli. Mol Syst Biol 11:781. https://doi.org/10.15252/msb.20145794.

13. Ignatov DV, Salina EG, Fursov MV, Skvortsov TA, Azhikina TL, Kaprelyants AS. 2015. Dormant non-culturable Mycobacterium tuberculosis retains stable low-abundant mRNA. BMC Genomics 16:954. https://doi.org/10 .1186/s12864-015-2197-6.

14. Tomcsanyi T, Apirion D. 1985. Processing enzyme ribonuclease E specifically cleaves RNA I. An inhibitor of primer formation in plasmid DNA synthesis. J Mol Biol 185:713–720. https://doi.org/10.1016/0022-2836 (85)90056-7.

15. Bouvet P, Belasco JG. 1992. Control of RNase E-mediated RNA degradation by 5'-terminal base pairing in E. coli. Nature 360:488–491. https:// doi.org/10.1038/360488a0.

16. McDowall KJ, Lin-Chao S, Cohen SN. 1994. A+U content rather than a particular nucleotide order determines the specificity of RNase E cleavage. J Biol Chem 269:10790–10796.

17. Apirion D, Gitelman DR. 1980. Decay of RNA in RNA processing mutants of Escherichia coli. Mol Gen Genet 177:339–343. https://doi.org/10.1007/ BF00267448.

18. Donovan WP, Kushner SR. 1986. Polynucleotide phosphorylase and ribonuclease II are required for cell viability and mRNA turnover in Escherichia coli K-12. Proc Natl Acad Sci U S A 83:120–124. https://doi .org/10.1073/pnas.83.1.120.

19. Py B, Causton H, Mudd EA, Higgins CF. 1994. A protein complex mediating mRNA degradation in Escherichia coli. Mol Microbiol 14:717–729. https://doi.org/10.1111/j.1365-2958.1994.tb01309.x.

20. Miczak A, Kaberdin VR, Wei CL, Lin-Chao S. 1996. Proteins associated with RNase E in a multicomponent ribonucleolytic complex. Proc Natl Acad Sci U S A 93:3865–3869. https://doi.org/10.1073/pnas.93.9.3865.

21. Py B, Higgins CF, Krisch HM, Carpousis AJ. 1996. A DEAD-box RNA helicase in the Escherichia coli RNA degradosome. Nature 381:169–172. https://doi.org/10.1038/381169a0.

22. Grunberg-Manago M. 1999. Messenger RNA stability and its role in control of gene expression in bacteria and phages. Annu Rev Genet 33:193–227. https://doi.org/10.1146/annurev.genet.33.1.193.

23. Carpousis AJ, Van Houwe G, Ehretsmann C, Krisch HM. 1994. Copurification of E. coli RNAase E and PNPase: evidence for a specific association between two enzymes important in RNA processing and degradation. Cell 76:889–900. https://doi.org/10.1016/0092-8674(94)90363-8.

24. Vanzo NF, Li YS, Py B, Blum E, Higgins CF, Raynal LC, Krisch HM, Carpousis AJ. 1998. Ribonuclease E organizes the protein interactions in the Escherichia coli RNA degradosome. Genes Dev 12:2770–2781. https://doi.org/10.1101/gad.12.17.2770.

25. Ait-Bara S, Carpousis AJ. 2010. Characterization of the RNA degradosome of Pseudoalteromonas haloplanktis: conservation of the RNase E-RhlB interaction in the gammaproteobacteria. J Bacteriol 192:5413–5423. https://doi.org/10.1128/JB.00592-10.

26. Commichau FM, Rothe FM, Herzberg C, Wagner E, Hellwig D, Lehnik-Habrink M, Hammer E, Völker U, Stülke J. 2009. Novel activities of glycolytic enzymes in *Bacillus subtilis*: interactions with essential proteins involved in mRNA processing. Mol Cell Proteomics 8:1350–1360. https://doi.org/10.1074/mcp.M800546-MCP200.

27. Roux CM, DeMuth JP, Dunman PM. 2011. Characterization of components of the *Staphylococcus aureus* mRNA degradosome holoenzyme-like complex. J Bacteriol 193:5520–5526. https://doi.org/10.1128/JB.05485-11.

28. Redko Y, Aubert S, Stachowicz A, Lenormand P, Namane A, Darfeuille F, Thibonnier M, De Reuse H. 2013. A minimal bacterial RNase J-based degradosome is associated with translating ribosomes. Nucleic Acids Res 41:288–301. https://doi.org/10.1093/nar/gks945.

29. Kovacs L, Csanadi A, Megyeri K, Kaberdin VR, Miczak A. 2005. Mycobacterial RNase E-associated proteins. Microbiol Immunol 49:1003–1007. https://doi.org/10.1111/j.1348-0421.2005.tb03697.x.

30. Csanadi A, Faludi I, Miczak A. 2009. MSMEG_4626 ribonuclease from *Mycobacterium smegmatis*. Mol Biol Rep 36:2341–2344. https://doi.org/10.1007/s11033-009-9454-1.

31. Tamura M, Moore CJ, Cohen SN. 2013. Nutrient dependence of RNase E essentiality in *Escherichia coli*. J Bacteriol 195:1133–1141. https://doi.org/10.1128/JB.01558-12.

32. Prud'homme-Genereux A, Beran RK, Iost I, Ramey CS, Mackie GA, Simons RW. 2004. Physical and functional interactions among RNase E, polynucleotide phosphorylase and the cold-shock protein, CsdA: evidence for a 'cold shock degradosome.' Mol Microbiol 54:1409–1421. https://doi.org/10.1111/j.1365-2958.2004.04360.x.

33. Regonesi ME, Del Favero M, Basilico F, Briani F, Benazzi L, Tortora P, Mauri P, Dehò G. 2006. Analysis of the *Escherichia coli* RNA degradosome composition by a proteomic approach. Biochimie 88:151–161. https://doi.org/10.1016/j.biochi.2005.07.012.

34. Chen C, Deutscher MP. 2005. Elevation of RNase R in response to multiple stress conditions. J Biol Chem 280:34393–34396. https://doi.org/10.1074/jbc.C500333200.

35. Chen C, Deutscher MP. 2010. RNase R is a highly unstable protein regulated by growth phase and stress. RNA 16:667–672. https://doi.org/10.1261/rna.1981010.

36. Kim KS, Manasherob R, Cohen SN. 2008. YmdB: a stress-responsive ribonuclease-binding regulator of *E. coli* RNase III activity. Genes Dev 22:3497–3508. https://doi.org/10.1101/gad.1729508.

37. Schubert OT, Ludwig C, Kogadeeva M, Zimmermann M, Rosenberger G, Gengenbacher M, Gillet LC, Collins BC, Rost HL, Kaufmann SH, Sauer U, Aebersold R. 2015. Absolute proteome composition and dynamics during dormancy and resuscitation of *Mycobacterium tuberculosis*. Cell Host Microbe 18:96–108. https://doi.org/10.1016/j.chom.2015.06.001.

38. Gao J, Lee K, Zhao M, Qiu J, Zhan X, Saxena A, Moore CJ, Cohen SN, Georgiou G. 2006. Differential modulation of *E. coli* mRNA abundance by inhibitory proteins that alter the composition of the degradosome. Mol Microbiol 61:394–406. https://doi.org/10.1111/j.1365-2958.2006.05246.x.

39. Iost I, Guillerez J, Dreyfus M. 1992. Bacteriophage T7 RNA polymerase travels far ahead of ribosomes *in vivo*. J Bacteriol 174:619–622. https://doi.org/10.1128/jb.174.2.619-622.1992.

40. Al-Husini N, Tomares DT, Bitar O, Childers WS, Schrader JM. 2018. α-Proteobacterial RNA degradosomes assemble liquid-liquid phase-separated RNP bodies. Mol Cell 71:1027–1039. https://doi.org/10.1016/j.molcel.2018.08.003.

41. Bayas CA, Wang J, Lee MK, Schrader JM, Shapiro L, Moerner WE. 2018. Spatial organization and dynamics of RNase E and ribosomes in *Caulobacter crescentus*. Proc Natl Acad Sci U S A 115:E3712–E3721. https://doi.org/10.1073/pnas.1721648115.

42. Gatewood ML, Jones GH. 2010. (p)ppGpp inhibits polynucleotide phosphorylase from *Streptomyces* but not from *Escherichia coli* and increases the stability of bulk mRNA in *Streptomyces coelicolor*. J Bacteriol 192:4275–4280. https://doi.org/10.1128/JB.00367-10.

43. Siculella L, Damiano F, di Summa R, Tredici SM, Alduina R, Gnoni GV, Alifano P. 2010. Guanosine 5'-diphosphate 3'-diphosphate (ppGpp) as a negative modulator of polynucleotide phosphorylase activity in a 'rare' actinomycete. Mol Microbiol 77:716–729. https://doi.org/10.1111/j.1365-2958.2010.07240.x.

44. Frederix M, Downie AJ. 2011. Quorum sensing: regulating the regulators. Adv Microb Physiol 58:23–80. https://doi.org/10.1016/B978-0-12-381043-4.00002-7.

45. Atkinson GC, Tenson T, Hauryliuk V. 2011. The RelA/SpoT homolog (RSH) superfamily: distribution and functional evolution of ppGpp synthetases and hydrolases across the tree of life. PLoS One 6:e23479. https://doi.org/10.1371/journal.pone.0023479.

46. Corrigan RM, Bellows LE, Wood A, Grundling A. 2016. ppGpp negatively impacts ribosome assembly affecting growth and antimicrobial tolerance in Gram-positive bacteria. Proc Natl Acad Sci U S A 113:E1710–E1719. https://doi.org/10.1073/pnas.1522179113.

47. Battesti A, Bouveret E. 2006. Acyl carrier protein/SpoT interaction, the switch linking SpoT-dependent stress response to fatty acid metabolism. Mol Microbiol 62:1048–1063. https://doi.org/10.1111/j.1365-2958.2006.05442.x.

48. Gentry DR, Hernandez VJ, Nguyen LH, Jensen DB, Cashel M. 1993. Synthesis of the stationary-phase sigma factor sigma s is positively regulated by ppGpp. J Bacteriol 175:7982–7989. https://doi.org/10.1128/jb.175.24.7982-7989.1993.

49. Chakraburtty R, Bibb M. 1997. The ppGpp synthetase gene (relA) of *Streptomyces coelicolor* A3(2) plays a conditional role in antibiotic production and morphological differentiation. J Bacteriol 179:5854–5861. https://doi.org/10.1128/jb.179.18.5854-5861.1997.

50. Martínez-Costa OH, Fernández-Moreno MA, Malpartida F. 1998. The relA/spoT-homologous gene in *Streptomyces coelicolor* encodes both ribosome-dependent (p)ppGpp-synthesizing and -degrading activities. J Bacteriol 180:4123–4132.

51. Artsimovitch I, Patlan V, Sekine S, Vassylyeva MN, Hosaka T, Ochi K, Yokoyama S, Vassylyev DG. 2004. Structural basis for transcription regulation by alarmone ppGpp. Cell 117:299–310. https://doi.org/10.1016/S0092-8674(04)00401-5.

52. Avarbock D, Avarbock A, Rubin H. 2000. Differential regulation of opposing Rel_Mtb activities by the aminoacylation state of a tRNA.ribosome.mRNA.Rel_Mtb complex. Biochemistry 39:11640–11648. https://doi.org/10.1021/bi001256k.

53. Bernstein JA, Khodursky AB, Lin PH, Lin-Chao S, Cohen SN. 2002. Global analysis of mRNA decay and abundance in *Escherichia coli* at single-gene resolution using two-color fluorescent DNA microarrays. Proc Natl Acad Sci U S A 99:9697–9702. https://doi.org/10.1073/pnas.112318199.

54. Nouaille S, Mondeil S, Finoux AL, Moulis C, Girbal L, Cocaign-Bousquet M. 2017. The stability of an mRNA is influenced by its concentration: a potential physical mechanism to regulate gene expression. Nucleic Acids Res 45:11711–11724. https://doi.org/10.1093/nar/gkx781.

55. Wayne LG, Hayes LG. 1996. An *in vitro* model for sequential study of shiftdown of *Mycobacterium tuberculosis* through two stages of nonreplicating persistence. Infect Immun 64:2062–2069.

56. Weiss LA, Stallings CL. 2013. Essential roles for *Mycobacterium tuberculosis* Rel beyond the production of (p)ppGpp. J Bacteriol 195:5629–5638. https://doi.org/10.1128/JB.00759-13.

57. Dahl JL, Arora K, Boshoff HI, Whiteford DC, Pacheco SA, Walsh OJ, Lau-Bonilla D, Davis WB, Garza AG. 2005. The relA homolog of *Mycobacterium smegmatis* affects cell appearance, viability, and gene expression. J Bacteriol 187:2439–2447. https://doi.org/10.1128/JB.187.7.2439-2447.2005.

58. Rock JM, Hopkins FF, Chavez A, Diallo M, Chase MR, Gerrick ER, Pritchard JR, Church GM, Rubin EJ, Sassetti CM, Schnappinger D, Fortune SM. 2017. Programmable transcriptional repression in mycobacteria using an orthogonal CRISPR interference platform. Nat Microbiol 2:16274. https://doi.org/10.1038/nmicrobiol.2016.274.

59. Shaila MS, Gopinathan KP, Ramakrishnan T. 1973. Protein synthesis in *Mycobacterium tuberculosis* H37Rv and the effect of streptomycin in streptomycin-susceptible and -resistant strains. Antimicrob Agents Chemother 4:205–213. https://doi.org/10.1128/aac.4.3.205.

60. Wu ML, Tan J, Dick T. 2015. Eagle effect in nonreplicating persister mycobacteria. Antimicrob Agents Chemother 59:7786–7789. https://doi.org/10.1128/AAC.01476-15.

61. Srivastava A, Asahara H, Zhang M, Zhang W, Liu H, Cui S, Jin Q, Chong S. 2016. Reconstitution of protein translation of *Mycobacterium* reveals functional conservation and divergence with the Gram-negative bacterium *Escherichia coli*. PLoS One 11:e0162020. https://doi.org/10.1371/journal.pone.0162020.

62. Wolfe AD, Hahn FE. 1965. Mode of action of chloramphenicol. IX. Effects of chloramphenicol upon a ribosomal amino acid polymerization system and its binding to bacterial ribosome. Biochim Biophys Acta 95:146–155. https://doi.org/10.1016/0005-2787(65)90219-4.

63. Yukioka M, Morisawa S. 1971. Enhancement of the phenylalanyl-oligonucleotide binding to the peptidyl recognition center of ribosomal peptidyltransferase and inhibition of the chloramphenicol binding to

ribosomes. Biochim Biophys Acta 254:304–315. https://doi.org/10.1016/0005-2787(71)90839-2.

64. Drainas D, Kalpaxis DL, Coutsogeorgopoulos C. 1987. Inhibition of ribosomal peptidyltransferase by chloramphenicol. Kinetic studies. Eur J Biochem 164:53–58. https://doi.org/10.1111/j.1432-1033.1987.tb10991.x.

65. Lopez PJ, Marchand I, Yarchuk O, Dreyfus M. 1998. Translation inhibitors stabilize *Escherichia coli* mRNAs independently of ribosome protection. Proc Natl Acad Sci U S A 95:6067–6072. https://doi.org/10.1073/pnas.95.11.6067.

66. Chan LY, Mugler CF, Heinrich S, Vallotton P, Weis K. 2018. Non-invasive measurement of mRNA decay reveals translation initiation as the major determinant of mRNA stability. Elife 7:e32536. https://doi.org/10.7554/eLife.32536.

67. Lakshmanan M, Xavier AS. 2013. Bedaquiline—the first ATP synthase inhibitor against multi drug resistant tuberculosis. J Young Pharm 5:112–115. https://doi.org/10.1016/j.jyp.2013.12.002.

68. Shetty A, Dick T. 2018. Mycobacterial cell wall synthesis inhibitors cause lethal ATP burst. Front Microbiol 9:1898. https://doi.org/10.3389/fmicb.2018.01898.

69. Rao SP, Alonso S, Rand L, Dick T, Pethe K. 2008. The protonmotive force is required for maintaining ATP homeostasis and viability of hypoxic, nonreplicating *Mycobacterium tuberculosis*. Proc Natl Acad Sci U S A 105:11945–11950. https://doi.org/10.1073/pnas.0711697105.

70. Eoh H, Rhee KY. 2013. Multifunctional essentiality of succinate metabolism in adaptation to hypoxia in *Mycobacterium tuberculosis*. Proc Natl Acad Sci U S A 110:6554–6559. https://doi.org/10.1073/pnas.1219375110.

71. Smith T, Wolff KA, Nguyen L. 2013. Molecular biology of drug resistance in *Mycobacterium tuberculosis*. Curr Top Microbiol Immunol 374:53–80. https://doi.org/10.1007/82_2012_279.

72. Kim JH, O'Brien KM, Sharma R, Boshoff HI, Rehren G, Chakraborty S, Wallach JB, Monteleone M, Wilson DJ, Aldrich CC, Barry CE, III, Rhee KY, Ehrt S, Schnappinger D. 2013. A genetic strategy to identify targets for the development of drugs that prevent bacterial persistence. Proc Natl Acad Sci U S A 110:19095–19100. https://doi.org/10.1073/pnas.1315860110.

73. Deb C, Lee CM, Dubey VS, Daniel J, Abomoelak B, Sirakova TD, Pawar S, Rogers L, Kolattukudy PE. 2009. A novel *in vitro* multiple-stress dormancy model for *Mycobacterium tuberculosis* generates a lipid-loaded, drug-tolerant, dormant pathogen. PLoS One 4:e6077. https://doi.org/10.1371/journal.pone.0006077.

74. Martini MC, Zhou Y, Sun H, Shell SS. 2019. Defining the transcriptional and post-transcriptional landscapes of *Mycobacterium smegmatis* in aerobic growth and hypoxia. Front Microbiol 10:591. https://doi.org/10.3389/fmicb.2019.00591.

75. Fan H, Conn AB, Williams PB, Diggs S, Hahm J, Gamper HB, Hou Y-M, O'Leary SE, Wang Y, Blaha GM. 2017. Transcription-translation coupling: direct interactions of RNA polymerase with ribosomes and ribosomal subunits. Nucleic Acids Res 45:11043–11055. https://doi.org/10.1093/nar/gkx719.

76. Zhang Y, Mooney RA, Grass JA, Sivaramakrishnan P, Herman C, Landick R, Wang JD. 2014. DksA guards elongating RNA polymerase against ribosome-stalling-induced arrest. Mol Cell 53:766–778. https://doi.org/10.1016/j.molcel.2014.02.005.

77. Miller OL, Jr, Hamkalo BA, Thomas CA. Jr. 1970. Visualization of bacterial genes in action. Science 169:392–395. https://doi.org/10.1126/science.169.3943.392.

78. Burmann BM, Schweimer K, Luo X, Wahl MC, Stitt BL, Gottesman ME, Rosch P. 2010. A NusE:NusG complex links transcription and translation. Science 328:501–504. https://doi.org/10.1126/science.1184953.

79. Proshkin S, Rahmouni AR, Mironov A, Nudler E. 2010. Cooperation between translating ribosomes and RNA polymerase in transcription elongation. Science 328:504–508. https://doi.org/10.1126/science.1184939.

80. Tedin K, Bremer H. 1992. Toxic effects of high levels of ppGpp in *Escherichia coli* are relieved by *rpoB* mutations. J Biol Chem 267:2337–2344.

81. Krasny L, Gourse RL. 2004. An alternative strategy for bacterial ribosome synthesis: *Bacillus subtilis* rRNA transcription regulation. EMBO J 23:4473–4483. https://doi.org/10.1038/sj.emboj.7600423.

82. Stallings CL, Stephanou NC, Chu L, Hochschild A, Nickels BE, Glickman MS. 2009. CarD is an essential regulator of rRNA transcription required for *Mycobacterium tuberculosis* persistence. Cell 138:146–159. https://doi.org/10.1016/j.cell.2009.04.041.

83. Esquerre T, Moisan A, Chiapello H, Arike L, Vilu R, Gaspin C, Cocaign-Bousquet M, Girbal L. 2015. Genome-wide investigation of mRNA lifetime determinants in *Escherichia coli* cells cultured at different growth rates. BMC Genomics 16:275. https://doi.org/10.1186/s12864-015-1482-8.

84. Farrow MF, Rubin EJ. 2008. Function of a mycobacterial major facilitator superfamily pump requires a membrane-associated lipoprotein. J Bacteriol 190:1783–1791. https://doi.org/10.1128/JB.01046-07.

85. Snapper SB, Melton RE, Mustafa S, Kieser T, Jacobs WR, Jr. 1990. Isolation and characterization of efficient plasmid transformation mutants of *Mycobacterium smegmatis*. Mol Microbiol 4:1911–1919. https://doi.org/10.1111/j.1365-2958.1990.tb02040.x.